Supplementay information for

Sustainable synthesis of hydroxyapatite-containing composites from eggshells for soil amendment applications

Letizia Castellini,[a] Alessia Giordana,[a] Mery Malandrino,[a] Lorenza Operti [a] and Giuseppina Cerrato* [a]

a) Dipatimento di Chimica, Università degli Studi di Torino, Via P. Giuria 7, 10125 Torino, Italy

List of Contents

1. **Experimental**
   Materials
   Synthetic procedures
   Characterization
   Green Chemistry Metrics (GMC) approach
   Ion Release Study
2. **Powder Diffraction Data**
   Figure S1. PXRD pattern of Hap-3
   Figure S2. PXRD pattern of Hap-2
   Figure S3. PXRD pattern of Hap-1
3. **Thermo-gravimetric analysis (TGA)**
   Figure S4. Thermo-gravimetric profile of Hap-1 and Hap-3
4. **GCM Results**
   Table S1. GCM results
   Figure S5. Category ranking of the samples with respect to improved resource use and reduced human and environmental hazard
5. **Ion Release study**
   Table S2. Quantities of calcium, phosphorous and potassium released from Hap-1
   Table S3. Quantities of calcium, phosphorous and potassium released from Hap-2
   Table S4. Quantities of calcium, phosphorous and potassium released from Hap-3
6. **Eggshells (ES) Characterization**
   Figure S6. ATR and Raman spectrum of ES
   Figure S7. PXRD pattern of ES
   Figure S8. SEM images of ES
   Table S5. Elemental composition of the samples from SEM-EDS analysis

1 - Experimental

Chemicals

The following reagents were used: calcium hydroxide ($Ca(OH)_2$; 95%) and L-(+)-ascorbic acid (HAsc; 98+ %) purchased from Thermo Scientific; ammonia (NH_3; p.a. 28-30%), phosphoric acid (H_3PO_4; 85%) and nitric acid (HNO_3; p.a. 65%) purchased from Sigma-Aldrich; potassium hydroxide (KOH; 85%) purchased from Fluka.

Synthetic procedures

Hydroxyapatite from commercial reagents (Hap-1) is used as a control sample and synthesized according to a previously reported precipitation method.[1] To synthesize 0.002 mol of Hap std, 0.02 mol of $Ca(OH)_2$ and 0.012 mol of H_3PO_4 were combined in a 10:6 molar ratio at rt. Briefly, $Ca(OH)_2$ was stirred in 40 ml of distilled water for 20 min until a homogeneous suspension was obtained. Then, H_3PO_4 (diluted with 40 ml of water) was slowly added dropwise, with continuous stirring. During the reaction, the pH was controlled and maintained above 10.5 by addition of ammonia solution, as necessary. The reagents were placed in an Erlenmeyer flask to minimize carbonate formation from reaction with atmospheric CO_2. The suspension was stirred for a further 2 hours and then allowed to stand overnight. The final product was filtered and dried under ambient conditions. The overall yield is 1.99 g (99.0%).

Characterization

Powder X-ray diffraction (PXRD) data were acquired using a X'Pert powder diffractometer operating in Bragg-Brentano geometry, equipped with a graphite crystal monochromator, and using Cu(Kα1) radiation (0.15406 nm) in the range 5-80° with step size of 0.02°. ATR-FTIR (Attenuated Total Reflection) spectra were using a Bruker VERTEX 70 spectrophotometer equipped with a Platinum ATR-QL diamond cell and a DTGS detector (32 scan, 4 cm^{-1} resolution). The general morphology/topography of various samples was assessed by means of scanning electron microscope operating with a field emission source (model: TESCAN S900G; source: Schottky type FEG; resolution: 0.7 nm at 15 keV in In-Beam SE mode), fitted with an EDS detector (Oxford EDS Ultim Max operating with Aztec software). Before the investigation, all samples were coated with Cr to enhance the conductivity. The specific surface areas (SSA) were determined from N_2 adsorption/desorption isotherms measured under subcritical conditions (77 K) using an ASAP 2020 instrument (Micromeritics). Sample degassing was performed at room temperature. SSA was calculated according to the B.E.T. model. Thermo-gravimetric analysis (TGA) was performed using TA Instruments (TGA Q500), under air flow, from rt to 700 °C at a heating rate of 10 °C/min. Raman spectra were acquired using a Bruker VERTEX 70 spectrometer equipped with the Ram II module, employing a Nd:YAG laser (λ = 1064 nm) and a high-sensitivity germanium diode detector (3000 scan, 4 cm^{-1} resolution, 125 mW laser power).

Green Chemistry Metrics (GMC) approach

For the GCM, a principle score (PS) was calculated for each of the 12 principles of green chemistry, following the equations reported by Krauder et al.[2] As the GCMs have been designed such that a lower PS indicates a greener option, the principle with the lowest PS is assigned a principle score rank (PSR) of 1, the next lowest a PSR of 2, and so on. In cases where PSR averages are tied, the corresponding alternatives are assigned the same rank. The mean PSRs within each category are then ranked to determine the category rank (CR).

Ion Release Study

Ca, K, P ions were quantified by inductively coupled plasma optical emission spectroscopy (ICP-OES). with radial viewing, performing triplicate measurements with a PerkinElmer Optima 7000 DV spectrometer. The wavelengths for P, Ca and K were 213.617, 317.933 and 769.896 nm, respectively. Calibrations were performed with standard solutions. The concentration of Ca, P and K on the Hap samples was determined in the same way by diluting 1:10 in water the solution obtained after digestion of 0.01 g of each sample in aqua regia.

---

1. Aina, V. *et al.* Magnesium- and strontium-co-substituted hydroxyapatite: the effects of doped-ions on the structure and chemico-physical properties. *J. Mater. Sci. Mater. Med.* **23**, 2867–2879 (2012).
2. DeVierno Kreuder, A. *et al.* A Method for Assessing Greener Alternatives between Chemical Products Following the 12 Principles of Green Chemistry. *ACS Sustain. Chem. Eng.* **5**, 2927–2935 (2017).

Synthesis of Hap-3: reaction scheme

$$\left.\begin{array}{c} \mathrm{CaCO_3 + 2\,H^+ \rightarrow\ Ca^{2+} +\ H_2O + CO_2} \\ \mathrm{HAsc\ \rightarrow H^+ +\ Asc^-} \end{array}\right] \quad \mathrm{CaCO_3 + 2\,HAsc\ \rightarrow Ca^{2+} +\ 2Asc^- + H_2\,O + CO_2}$$

$$\left.\begin{array}{c} \mathrm{HAsc \rightarrow DHA + 2H^+ + 2\,e^-} \\ \mathrm{CO_2 + 2H^+ + 2\,e^- \rightarrow H_2\,C_2O_4} \end{array}\right] \quad \mathrm{CO_2 + HAsc \rightarrow H_2\,C_2O_4 + DHA}$$

$\mathrm{H_2C_2O_4}$ = Oxalic acid
DHA = Dehydroascorbic acid

2 - Powder diffraction data

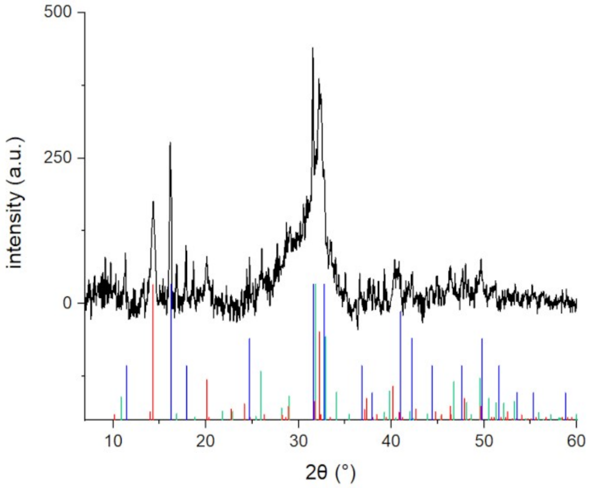

Figure S1.PXRD pattern of Hap-3 (black line) compared to references weddellite (ICDD card PDF N. 00-017-0541) (red line), whewellite (ICDD card PDF No. 00-014-0769) (blue line) and Hap (ICDD card PDF N. 01-084-1998) (green line).

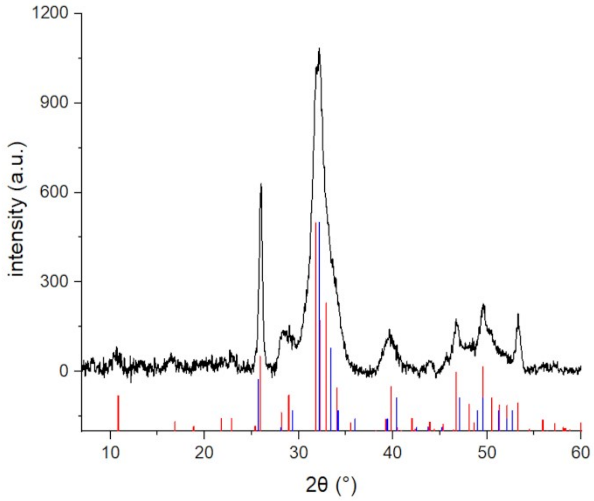

Figure S2. PXRD pattern of Hap-2 (black line) compared to the references carbonated-substituted Hap (ICDD card PDF No. 00-019-0272) (blue line) and Hap (ICDD card PDF N. 01-084-1998) (red line)

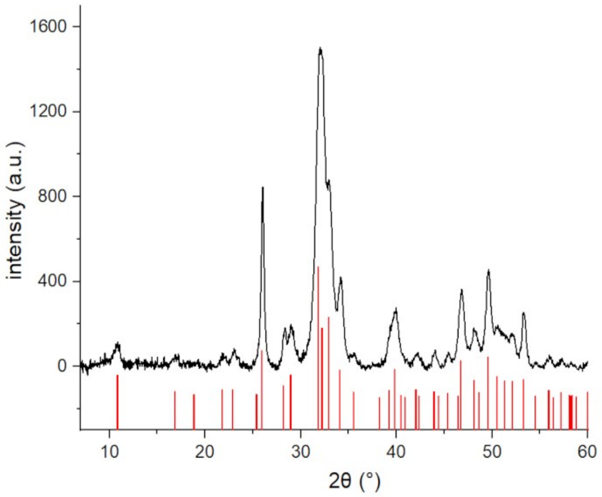

Figure S3. PXRD pattern of Hap-1 (black line) compared to the reference Hap (ICDD card PDF N. 01-084-1998) (red line)

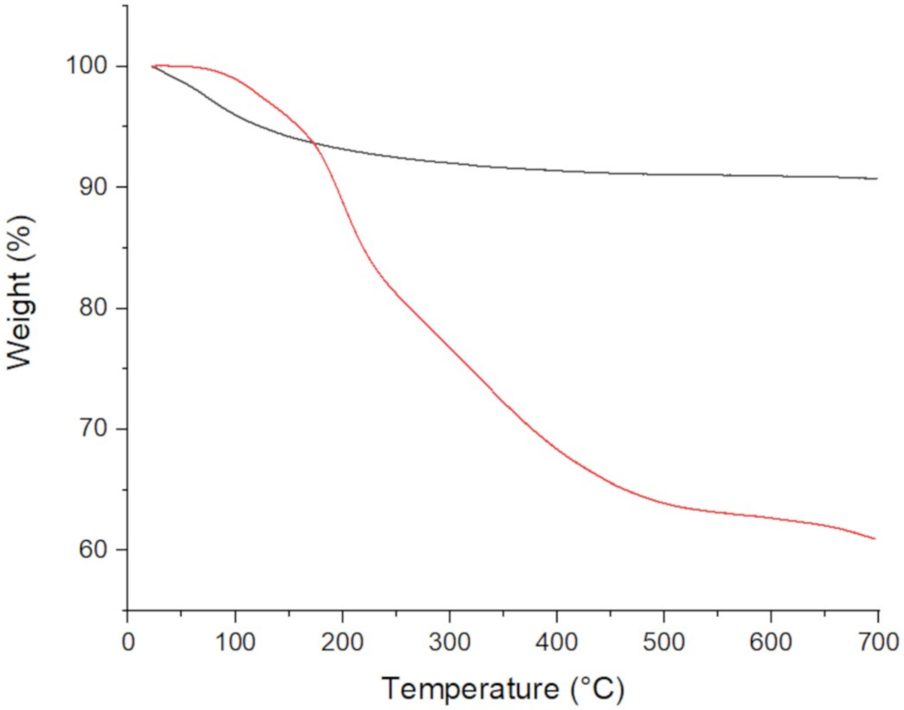

Figure S4. Thermo-gravimetric profile of Hap-1 (black line) and Hap-3 (red line).

3 – Thermo-gravimetric analysis (TGA)

4 – GCM Results

Table S1. GCM results

Category and related principles	Hap-1	Hap-2	Hap-3	Hap-4
Improved resource use				
Category Rank	*2*	*4*	*3*	*1*
Category PSR	1.5	2.7	2.2	1.2
PS P1	71	107	79	31
PSR P1	2	4	3	1
PS P2	49	77	59	23
PSR P2	2	4	3	1
PS P7	80	316	226	121
PSR P7	1	4	3	2
PS P8	0	0	0	0
PSR P8	1	1	1	1
PS P9	1	1	1	1
PSR P9	1	1	1	1
PS P11	0.7	0.7	0.7	0.1
PSR P11	2	2	2	1
Increased energy efficiency				
Category Rank	*1*	*3*	*2*	*4*
Category PSR	1	3	2	4
PS P6	41	111	60	151
PSR P6	1	3	2	4
Reduced human and environmental hazards				
Category Rank	*1*	*3*	*2*	*2*
Category PSR	1.2	2.8	1.8	1.8
PS P3	7	25	9	12
PSR P3	1	4	2	3
PS P4	1	1	1	1
PSR P4	1	1	1	1
PS P5	47	83	62	21
PSR P5	2	4	3	1
PS P10	1	1	1	1
PSR P10	1	1	1	1
PS P12	7	24	8	12
PSR P12	1	4	2	3

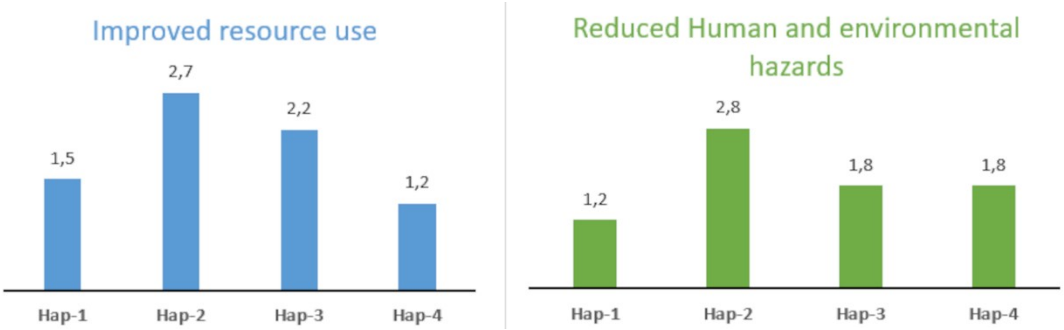

Figure S5. Bar graph showing the category ranking of the samples (Hap-1, Hap-2, Hap-3 and Hap-4) with respect to improved resource use (blue bars one the left) and Reduced human and environmental hazard (green bars on the right).

5 – Ions Release Study

Table S2. Quantities of calcium, phosphorous and potassium released from Hap-1

Time (h)	Ca (mg) [a]	Ca%[b]	P (mg) [a]	P%[b]	K (mg) [a]	K%[b]
24	0.011±0.001	0.02%	0.234±0.002	0.73%	0.009±0.001	0.14%
48	0.036±0.001	0.06%	0.077±0.001	0.24%	0.008±0.001	0.12%
72	0.043±0.001	0.07%	0.047±0.001	0.15%	0.006±0.001	0.09%
96	0.059±0.003	0.1%	0.046±0.001	0.14%	0.003±0.001	0.05%
168	0.048±0.001	0.08%	0.041±0.001	0.13%	0.002 ±0.001	0.03%

[a] mg of ions released in water and associated measurement error; [b] wt% of ions released/total.

Table S3. Quantities of calcium, phosphorous and potassium released from Hap-2

Time (h)	Ca (mg) [a]	Ca%[b]	P (mg) [a]	P%[b]	K (mg) [a]	K%[b]
24	0.045 ±0.003	0.11%	0.169 ±0.003	0.81%	6.23 ±0.04	32%
48	0.034 ±0.003	0.08%	0.128 ±0.003	0.61%	0.53 ±0.02	2.7%
72	0.060 ±0.002	0.14%	0.054 ±0.001	0.26%	0.08 ±0.01	0.42%
96	0.074 ±0.013	0.17%	0.045 ±0.006	0.21%	0.012 ±0.001	0.06%
168	0.087 ±0.009	0.21%	0.048 ±0.002	0.23%	0.009 ±0.002	0.05%

[a] mg of ions released in water and associated measurement error; [b] wt% of ions released/total.

Table S4. Quantities of calcium, phosphorous and potassium released from Hap-3

Time (h)	Ca (mg) [a]	Ca%[b]	P (mg) [a]	P%[b]	K (mg) [a]	K%[b]
24	0.308 ±0.001	0.86%	0.170 ±0.002	1.2	4.39 ±0.08	45%
48	0.248 ±0.002	0.69%	0.466 ±0.005	3.2%	0.71 ±0.04	7.2%
72	0.29 ±0.02	0.79%	0.220 ±0.015	1.5%	0.14 ±0.01	1.4%
96	0.244 ±0.011	0.68%	0.159 ±0.009	1.1%	0.025 ±0.001	0.26%
168	0.275 ±0.008	0.77%	0.182 ±0.007	1.2%	0.019 ±0.002	0.20%

[a] mg of ions released in water and associated measurement error. [b] wt% of ions released/total

6 – Eggshells (ES) Characterization

Characterization data of the ES employed in this study are analogous to literature. Signals in the ATR-FTIR spectrum are attributable to carbonate modes. Powder diffraction pattern indicate that ES are composed by $CaCO_3$ in the form of calcite (ICDD card PDF N. 01-072-1652), as confirmed by the characteristic Raman signals at 1088, 715, 278 and 155 cm^{-1}. Elemental analysis (by EDS) shows a trace amount of Mg (0.3%).

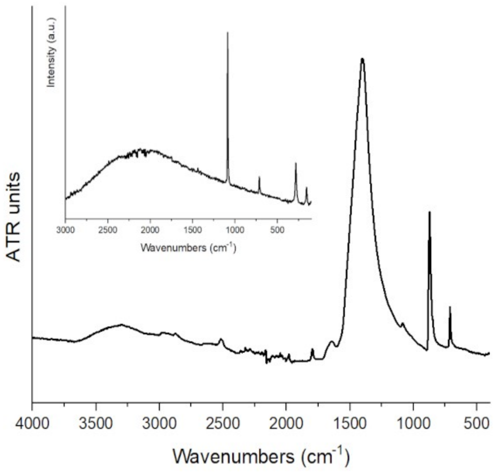

Figure S6. ATR-FTIR and Raman (in the inset) spectra of ES.

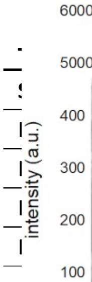

and Eggshells powders from SEM-EDS analysis

lg (wt%)
-
-
-
0.3

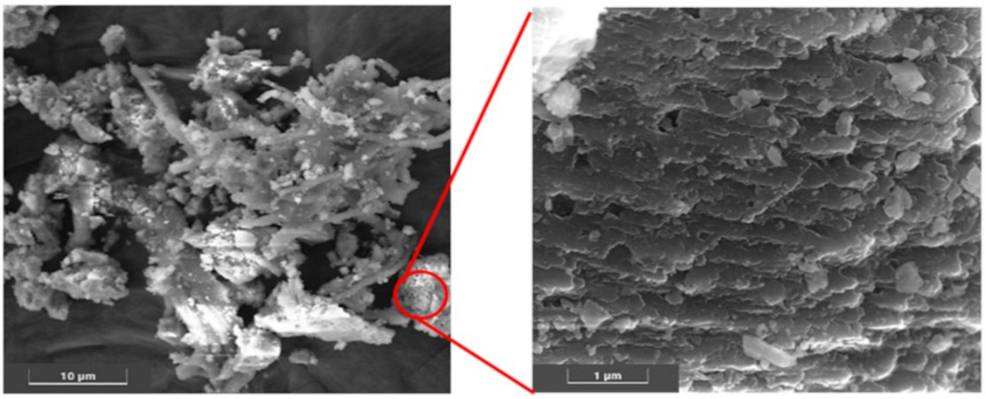

Figure 52) (red line).

Figure S8. SEM images of ES.